Journal of Biomedical Optics

BiomedicalOptics.SPIEDigitalLibrary.org

Reversibly switchable fluorescence microscopy with enhanced resolution and image contrast

Junjie Yao
Daria M. Shcherbakova
Chiye Li
Arie Krumholz
Ramon A. Lorca
Erin Reinl
Sarah K. England
Vladislav V. Verkhusha
Lihong V. Wang

SPIE.

Reversibly switchable fluorescence microscopy with enhanced resolution and image contrast

Junjie Yao,[a] Daria M. Shcherbakova,[b] Chiye Li,[a] Arie Krumholz,[a] Ramon A. Lorca,[c] Erin Reinl,[c] Sarah K. England,[c] Vladislav V. Verkhusha,[b,*] and Lihong V. Wang[a,*]
[a]Washington University, Department of Biomedical Engineering, St. Louis, Missouri 63130, United States
[b]Albert Einstein College of Medicine, Gruss-Lipper Biophotonics Center, Department of Anatomy and Structural Biology, Bronx, New York 10461, United States
[c]Washington University School of Medicine, Department of Obstetrics and Gynecology, St. Louis, Missouri 63130, United States

Abstract. Confocal microscopy with optical sectioning has revolutionized biological studies by providing sharper images than conventional optical microscopy. Here, we introduce a fluorescence imaging method with enhanced resolution and imaging contrast, which can be implemented using a commercial confocal microscope setup. This approach, called the reversibly switchable photo-imprint microscopy (rsPIM), is based on the switching dynamics of reversibly switchable fluorophores. When the fluorophores are switched from the bright (ON) state to the dark (OFF) state, their switching rate carries the information about the local excitation light intensity. In rsPIM, a polynomial function is used to fit the fluorescence signal decay during the transition. The extracted high-order coefficient highlights the signal contribution from the center of the excitation volume, and thus sharpens the resolution in all dimensions. In particular, out-of-focus signals are greatly blocked for large targets, and thus the image contrast is considerably enhanced. Notably, since the fluorophores can be cycled between the ON and OFF states, the whole imaging process can be repeated. RsPIM imaging with enhanced image contrast was demonstrated in both fixed and live cells using a reversibly switchable synthetic dye and a genetically encoded red fluorescent protein. Since rsPIM does not require the modification of commercial microscope systems, it may provide a simple and cost-effective solution for subdiffraction imaging of live cells. [DOI: 10.1117/1.JBO.19.8.086018]

Keywords: rsTagRFP; subdiffraction imaging; reversibly switchable fluorophore; contrast enhancement.

Paper 140362R received Jun. 9, 2014; revised manuscript received Jul. 31, 2014; accepted for publication Jul. 31, 2014; published online Aug. 21, 2014.

1 Introduction

Subdiffraction imaging has opened new possibilities for fundamental biological studies.[1] With resolutions finer than the optical diffraction limit, subdiffraction imaging has enabled the observations of cellular and subcellular structures and processes which are unresolvable with conventional microscopes. Generally, subdiffraction techniques fall into two broad categories: ensemble imaging methods with patterned illumination, such as stimulated emission depletion microscopy,[2] dynamic saturation optical microscopy,[3,4] reversible saturable optical fluorescence transitions imaging (RESOLFT),[5] and structured illumination microscopy;[6] and single-molecule imaging and localization methods, such as (fluorescence) photoactivation localization microscopy [(F)PALM][7,8] and stochastic optical reconstruction microscopy (STORM).[9]

Recently, we have developed a new subdiffraction imaging method by integrating the intensity-dependent photobleaching effect into absorption-based photoacoustic microscopy.[10] A lateral resolution of 80 nm has been demonstrated using photobleaching of gold nanoparticles. The axial resolution is also improved by effectively removing the out-of-focus signal contributions. Optical sectioning for large targets, which is otherwise missing in wide-field detection photoacoustic microscopy, has been accomplished. More importantly, this method is generic and can be applied to both fluorescent and nonfluorescent targets. Following its first demonstration in photoacoustic imaging, this method has been adopted in fluorescence imaging, including confocal microscopy, two-photon microscopy, wide-field microscopy, and light-sheet microscopy.[11–13] However, photobleaching is a nonreversible process and will inevitably perturb the original contrast. Therefore, photobleaching-based subdiffraction imaging is not suitable for biological studies where permanent change is not tolerable.

Instead of permanent photobleaching, reversibly switchable fluorophores, including reversibly switchable fluorescent proteins (rsFPs) and synthetic dyes, can be switched between fluorescent (ON) and nonfluorescent (OFF) states when illuminated at appropriate wavelengths.[14,15] In recent years, rsFPs, such as green Dronpa,[16] reversibly switchable enhanced green fluorescent protein,[17] and rsTagRFP,[18,19] have been applied to fluorescence imaging with enhanced spatial resolution in (F)PALM/STORM,[20–22] RESOLFT,[5] and photochromic stochastic optical fluctuation imaging (pcSOFI).[23] They have also been used to enhance weak signals in optical lock-in detection imaging (OLID).[24] Most recently, two similar techniques, such as multiphoton deactivation imaging (MPDI) and multiphoton activation imaging (MPAI),[25] were demonstrated on tissue phantoms labeled with rsFPs. MPDI and MPAI have dramatically improved the image contrast, taking advantage of the switching rate difference of the rsFPs in and out of the optical focus. However, many of the existing subdiffraction imaging methods based on rsFPs rely solely on the two extreme ON and OFF

*Address all correspondence to: Vladislav V. Verkhusha, E-mail: vladislav.verkhusha@einstein.yu.edu; Lihong V. Wang, E-mail: lhwang@biomed.wustl.edu

0091-3286/2014/$25.00 © 2014 SPIE

states, while the switching process, which takes most of the imaging time, is not utilized. In addition, some of the subdiffraction imaging methods need to robustly cycle the rsFPs for hundreds of times, which have limited the choices of usable fluorophores.[5]

Here, we propose a simple lossless subdiffraction imaging method by extending the previous photobleaching-based techniques with rsFPs. We termed this technique "reversibly switchable photo-imprint microscopy (rsPIM)." Different from the other rsFP-based methods, in rsPIM, the resolution enhancement is achieved by scrutinizing the switching process between the two extreme states. We have demonstrated that the switching rates of rsFPs between ON and OFF states strongly depend on the illumination intensity, which enables spatial trimming of the excitation volume to a subdiffraction size. In addition, our results have shown that optical sectioning can be enhanced by using the dependence of the switching rate on the axial position. The major advantage of our method is the technical simplicity, where a commercial "off-the-shelf" imaging system is used without any engineering modifications. Since no complex illumination pattern or repeated switching of rsFPs is needed, it has eliminated the stringent requirements of precise optical alignment and robustness of the fluorophores against photobleaching.

2 Principle of Reversibly Switchable Photo-Imprint Microscopy Imaging

The principle of rsPIM is shown in Fig. 1(a). rsPIM is implemented on a commercial confocal microscope (Olympus FV1000). When ON-state fluorophores are excited by a Gaussian beam at the switching-off wavelength, the generated fluorescence signal is a summation of the contributions from all fluorophores inside the excitation volume [Fig. 1(a)]. During the excitation, the fluorophores inside the excitation volume are switched off at a rate dependent on the spatial distribution of the local excitation intensity [Fig. 1(a)]. The switching-off rate typically has a power dependence of one on the excitation intensity in one-photon absorption, and at least two in two-photon absorption.[13] Therefore, the fluorescence signal in the center of the excitation volume decays faster than that in the periphery. As a result, the fluorescence signal decay not only reflects the excitation intensity profile, but also incorporates the fluorophore switching-off distribution [Fig. 1(a)], which depends nonlinearly on the local excitation intensity. Fitting the resultant fluorescence signal decay shows that the fluorophores in the center contribute more to the high-order coefficients of the polynomial fitting than those in the periphery. Therefore, extracting the high-order coefficients can sharpen the associated excitation volume in all dimensions.

For the lateral resolution, the schematic of this concept is presented in Fig. 1(b). The effective lateral point spread function (PSF) [Fig. 1(b), right panel] of the system is sharper than the initial lateral excitation PSF [Fig. 1(b), left panel] by a factor of $\sqrt{2+bk}$, where b is the power dependence of the switching-off rate on the excitation intensity, and k is the order of polynomial fitting of the signal decay.[10] In comparison, the lateral PSF of confocal microscopy is sharper than the initial excitation PSF by a factor of $\sqrt{2}$. The detailed mathematic derivations for the resolution enhancement in rsPIM can be found in Refs. 10 and 13

In addition to lateral resolution improvement, the nonlinear nature of the rsPIM signal enhances optical sectioning in the axial direction, which is of particular interest for large (or planar) targets. A simple illustration is shown in Fig. 1(c). Compared with the in-focus fluorophores, the out-of-focus fluorophores are less affected during the switching-off process. Therefore, high-order coefficients extracted from the polynomial fitting of the signal decay will contain few out-of-focus contributions, and thus will sharpen the optical focal zone. Like the lateral resolution enhancement, the sectioning strength of rsPIM is determined by the power dependence of the switching-off rate on the excitation intensity. For point targets, rsPIM can improve the axial resolution by a factor of $1/\sqrt{2^{1/(2+bk)}-1}$ over conventional microscopy. For large targets, rsPIM can improve the axial resolution by a factor of $1/\sqrt{2^{1/(1+bk)}-1}$ over confocal microscopy.[10]

3 Experimental Methods

To demonstrate the above principle, rsPIM imaging was performed on fixed cells stained by a reversibly switchable synthetic dye and live cells expressing a genetically encoded red fluorescent protein. A fluorescent dye Alexa Fluor 647 (AF647) was first exploited to demonstrate our method on fixed cells. AF647 is a carbocyanine-based synthetic probe that can be reversibly switched on and off at 405 and 635 nm, respectively.[22] In addition to demonstrating rsPIM with dyes, we further utilized this technique with genetically encoded rsTagRFP on live cells. rsTagRFP can be switched on and off at 440 and 570 nm, respectively.[26]

3.1 *Fluorescence Imaging*

After the sample was labeled with AF647, fluorescence images were acquired on an Olympus Fluoview FV1000 microscope (Olympus America Inc., Center Valley, Pennsylvania)[27] with an oil immersion objective lens (PlanApo, 100×, NA = 1.4, Nikon Instruments Inc., Melville, New York) [Fig. 1(d)]. For confocal imaging, a 635-nm continuous wave laser was used for excitation and switching the dye to the OFF state. The fluorescence light was selected by a 655 to 755 nm barrier filter. A 405-nm continuous wave laser activated the dye to the ON state. The exposure time for each pixel was 4 μs, and the scanning step size was 0.07 μm.

For confocal imaging of rsTagRFP, a 460-nm blue laser was used for switching the proteins to the ON state and a 530-nm green laser was used for switching the proteins to the OFF state. A 570 to 625-nm barrier filter selected the fluorescence light during the switching-off process. The exposure time for each pixel was 8 μs, and the scanning step size was 0.09 μm. The other imaging parameters were the same as those used in AF647 imaging.

For wide-field imaging of rsTagRFP bacterial cells, the samples were excited by a mercury lamp and imaged by the same oil immersion objective. Fluorescence images were acquired using a 512×512 pixels charge coupled device camera (DV412-BV, Andor Technology, United Kingdom). The excitation and emission filters were the same as those used in the confocal imaging of rsTagRFP.

3.2 *Data Processing for Reversibly Switchable Photo-Imprint Microscopy*

In brief, a simple threshold was first applied to the image to significantly reduce the processing time. Only the pixels with a signal decrease of more than 1% during the switching-off were further processed. At each eligible pixel, the signal decay was fitted by a polynomial function of 3 deg with not more than 1000

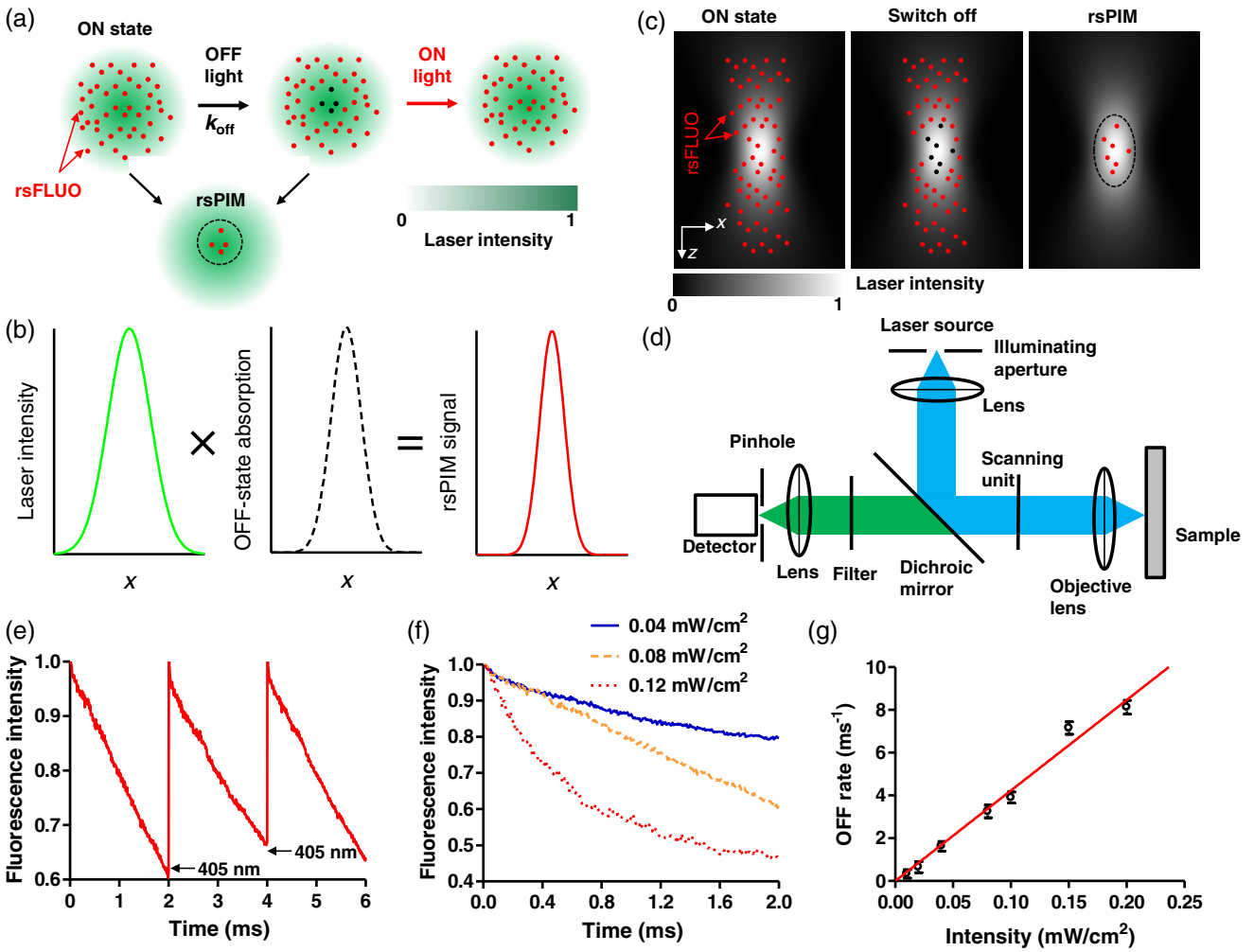

Fig. 1 Characterization of reversibly switchable photo-imprint microscopy (rsPIM). (a) Principle of rsPIM imaging. Within the diffraction-limited excitation spot, the ON-state fluorophores are switched to the OFF state, where the switching-off rate (k_{off}) increases linearly with the local excitation intensity. Such intensity dependence results in an inhomogeneous reduction of the fluorescence signal across the excitation volume, with the center decaying faster than the periphery. By fitting the switching-off dynamics, rsPIM can sharpen the effective excitation volume, and thus improve the imaging resolution. The whole process can be repeated by cycling the fluorophores between the ON and OFF states. (b) Illustration of the lateral resolution enhancement by rsPIM. For the first-order approximation, the effective point spread function (PSF) is the product of the excitation PSF and the switching-off profile. (c) Illustration of the axial resolution enhancement provided by rsPIM. The switching-off rate dependence on the axial position largely removes the out-of-focus contributions. (d) Schematic of the confocal microcopy. (e) Time course of Alexa Fluor 647 (AF647) fluorescence signal intensity during three consecutive switching cycles. The fluorescence was normalized to the starting point of the first cycle. (f) Time courses of the switching-off dynamics with three representative excitation intensities measured at the backaperture of the objective. (g) Linear dependence of the switching-off rate on the excitation light intensity.

iterations. The extracted third-order coefficients formed an rsPIM image, while the un-fitted pixels were set to zero. All the confocal images acquired during a switching cycle were averaged and used as a comparison.

In OLID imaging, the averaged signal intensity within the cell region during three switching cycles was used as the reference signal. Each pixel was correlated with the reference signal, and the correlation coefficients formed an OLID image.

All data were processed using MATLAB® R2010b. In particular, the polynomial fitting of the signal decay in rsPIM was performed by using the signal processing toolbox. Parallel computation was performed since each pixel was completely independent. By using an eight-core computer station at 3.4 GHz, the total processing time was less than 10 s.

3.3 *Cell Staining with Alexa Fluor 647*

Slides with NIH 3T3 fibroblast cells adhering to the glass surface were rinsed by phosphate buffered saline (PBS). The slides were fixed in 4% formaldehyde for 20 min and again washed with PBS. The cells were permeabilized for 2 min in a buffer made of 0.5% (v/v) Triton X-100, 3% (w/v) bovine serum albumin (BSA) in the PBS. Then blocking was performed by using a blocking buffer [0.2% (v/v) Triton X-100, 3% (w/v) BSA in PBS] for 1 h to reduce the nonspecific binding of the antibodies (Abs). The samples were first incubated with 2 μg/ml primary α-tubulin mouse monoclonal Abs for 45 min and washed with blocking buffer. Then, 2.5 μg/ml secondary AF647 goat antimouse Abs was added to the sample for 45 min and washed

with blocking buffer. Next the signal was amplified by using 2.5 μg/ml tertiary AF647 rabbit antigoat Abs. After staining, the samples were fixed again. Imaging buffer [10% (w/v) glucose, 0.5 mg/ml glucose oxidase, 40 μg/ml catalase, 0.7 mg/ml cysteamine in Tris-HCl, pH 8.5] was added to the fixed slides.

3.4 *Plasmids and Expressing Bacteria*

Unless otherwise listed, all cells and molecular biology supplies were purchased from Life Technologies (Carlsbad, California). A gene of rsTagRFP was cloned into a pBAD/His-B vector as the *BglII-EcoRI* fragment and expressed in an LMG194 bacterial host. Both the prsTagRFP-H2B and prsTagRFP-β-actin plasmids for mammalian expression were constructed by swapping the rsTagRFP gene for an mTagBFP2 gene in the respective mTagBFP2 plasmids.[28]

3.5 *Mammalian Cell Culture*

NIH 3T3 fibroblast cells were cultured in Dulbecco's modified eagle medium (DMEM) supplemented with 10% fetal bovine serum (FBS), 2 mM glutamine, 100 unites/ml penicillin, and 100 μg/ml streptomycin. Cells were incubated at 37°C in 5% CO_2 and divided every 72 h.

HeLa epithelial cells were grown to 60%–80% confluency in DMEM/F12 supplemented with 10% FBS and 50 μg/ml gentamicin. Cells were transiently transfected with 1 μg/ml of plasmids encoding both the prsTagRFP-H2B and prsTagRFP-β-actin fusion constructs using Lipofectamine 2000 according to the manufacturer's directions. Cells were plated on glass bottom dishes (MatTek Corporation, Ashland, Massachusetts) 24 h after transfection and imaged 48 h post-transfection in PBS supplied with 1% BSA.

4 Results

4.1 *Reversibly Switchable Photo-Imprint Microscopy with Reversibly Switchable Synthetic Dye*

We first investigated the switching dynamics of AF647. A glass microtube filled with AF647 was repeatedly imaged and cycled with different light intensities. The fluorescence intensity was decreased during the excitation at 635 nm (i.e., switching off), and was robustly recovered after excitation at 405 nm (i.e., switching on) [Fig. 1(e)]. The fluorescence intensity decay rate was increased in linear proportion to the excitation intensity at 635 nm, which suggests a one-photon absorption process [Figs. 1(f) and 1(g)]. These phantom results laid the foundations for the subdiffraction imaging by rsPIM.

A sharp edge coated by AF647 was used to quantify the lateral resolution of rsPIM. At each pixel, the signal decay was fitted by a polynomial function of 3 deg. Here, the optimal polynomial order was largely determined by the available signal-to-noise ratio (SNR). The extracted third-order coefficients formed an rsPIM image, while the averaged signal intensity formed a confocal microscopy image. For both images, the line spread function (LSF) was extracted from the measured edge-spread function [Fig. 2(a)]. The full width at half maximum (FWHM) of the LSF suggests a lateral resolution of 230 nm for confocal microscopy and 130 nm for rsPIM, a 1.7-fold improvement. Such an improvement was close to the theoretical value of 1.6 with $b = 1$ and $k = 3$. To demonstrate the imaging performance, confocal microscopy and rsPIM were applied to image a monolayer of 500-nm diameter densely packed AF647-stained microbeads [Fig. 2(b)]. The images show that the microbeads were better resolved by rsPIM, which confirmed the lateral resolution improvement. In addition to fitting the signal decaying by a polynomial function, other image processing methods can also be used to extract the signal contributions from the central region of the excitation spot. For example, we can fit the signal decay curve by a set of exponential functions with different time constants, where the smallest time constants correspond to the signal contributions from the center region.[28]

The lateral resolution enhancement of rsPIM was further demonstrated on fixed NIH 3T3 fibroblast cells stained with AF647-labeled Abs against α-tubulin [Fig. 2(c)]. Both confocal and rsPIM images were performed with a single switching cycle. Compared with the confocal microscopy image, the rsPIM image shows superior resolution in the subcellular features. Moreover, due to enhanced optical sectioning, the imaging contrast between the cytoplasm and cell nucleus has improved 22-fold, from 3.8 in confocal microscopy to 83.3 in rsPIM [Fig. 2(e)].

As a comparison, OLID imaging was also performed with three switching cycles [Fig. 2(d)]. Compared with the rsPIM image, the OLID image shows a significantly improved visibility of the weak signals. However, the imaging contrast between the cytoplasm and cell nucleus was degraded. Because OLID calculates the correlation coefficient of each image pixel with a given reference signal, it selectively boosts the pixels that resemble the cycling pattern of the reference signal. Here, it is important to point out that OLID is very powerful for distinguishing the switching pixels from the nonswitching background pixels and the simple OLID imaging process performed here may not be optimized to match the state-of-the-art OLID technique due to our lack of expertise.[29] However, we want to emphasize that OLID is not as sensitive to the signal switching rate as rsPIM [Fig. 2(e)].[24] Therefore, OLID does not have subdiffraction imaging capability.

4.2 *Reversibly Switchable Photo-Imprint Microscopy Using Reversibly Switchable Fluorescent Protein in Live Cells*

Here, we demonstrated the resolution enhancement of rsPIM in live cells by using rsTagRFP. To study the switching dynamics of rsTagRFP, streaks of LMG194 bacterial cells expressing rsTagRFP were imaged with conventional wide-field fluorescence microscopy [Fig. 3(a)]. Three switching cycles were performed, and each cycle lasted for 300 s (switching on, 150 s; switching off, 150 s). After being switched off, about 90% of the rsTagRFP molecules were switched back to the ON state, which confirmed the high photostability of rsTagRFP [Fig. 3(b)]. The switching-off rate of rsTagRFP linearly depends on the excitation intensity.[15] As an example, three representative regions were intentionally selected in Fig. 3(a), where region B was believed to be from the focal plane and regions A and C were from out-of-focus planes, based on the feature blurring of the three regions. As shown in Fig. 3(c), the switching-off rates of regions A, B, and C are 0.03 s^{-1}, 0.007 s^{-1}, and 0.015 s^{-1}, respectively, reflecting the excitation intensity heterogeneity along the axial beam axis.

Taking advantage of this axial dependence of the switching-off rate, rsPIM can efficiently block the signal contributions from out-of-focus planes. By fitting the signal decay with polynomial functions, the third-order coefficients can be extracted which represent signal components with faster decay rates,

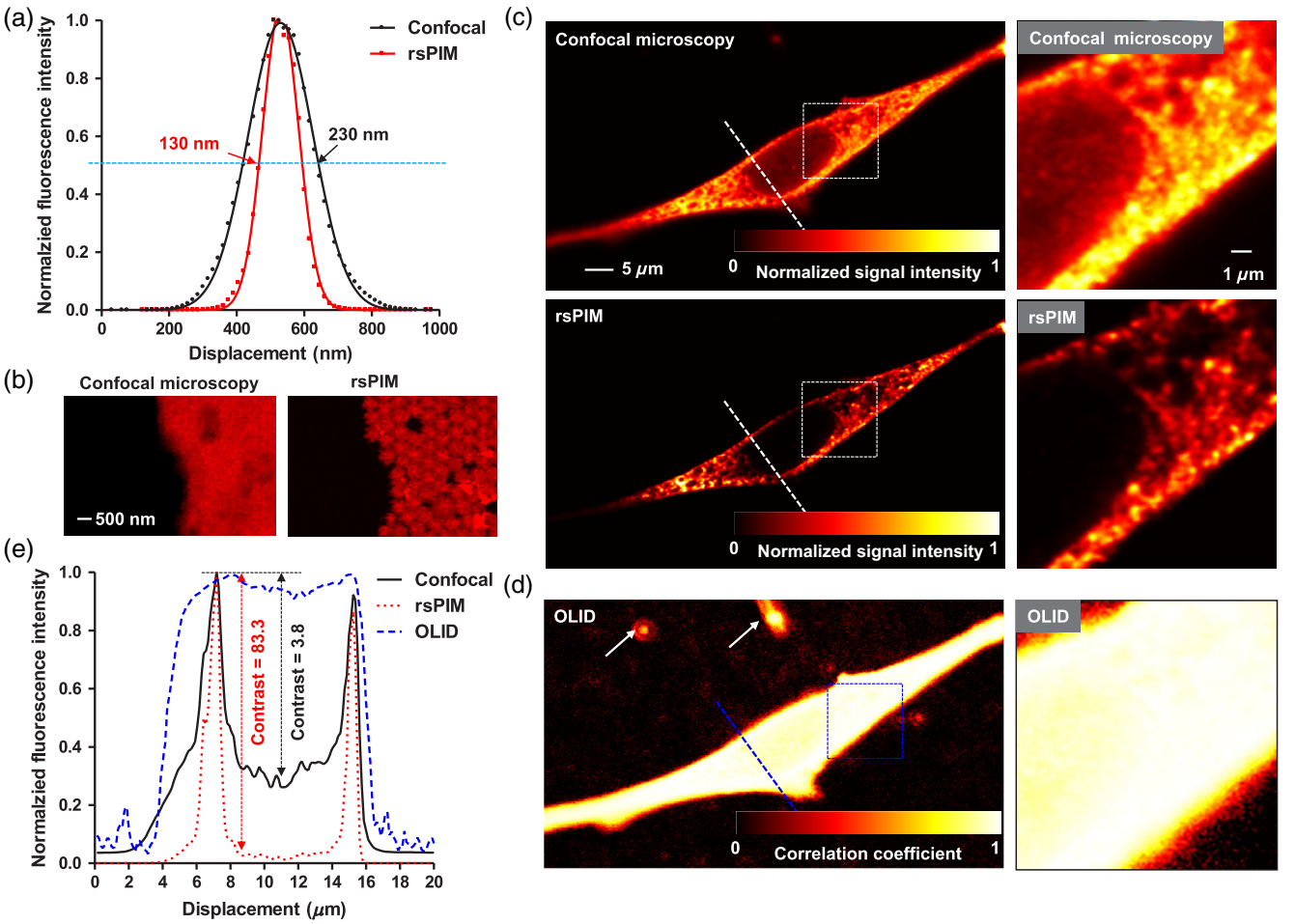

Fig. 2 Lateral resolution enhancement by reversibly switchable photo-imprint microscopy (rsPIM). (a) The line spread function (LSF) was extracted from the measured edge-spread function of a sharp edge coated by Alexa Fluor 647 (AF647). Dots: LSF extracted at each pixel; Solid lines: Gaussian fitting. The full width at half maximum (FWHM) of the LSF suggests a lateral resolution of 230 nm for confocal microscopy and 130 nm for rsPIM, which is a 1.7-fold improvement. (b) Confocal microscopy (left) and rsPIM of 500-nm microbeads stained with AF647, where single beads can be better resolved by rsPIM. (c) Confocal microscopy and rsPIM of the fixed NIH 3T3 fibroblast cells stained with AF647-labeled Abs against α-tubulin. The rsPIM image shows a better resolution and a cytoplasm-nucleus contrast than the confocal microscopy image. Right column: close-ups of the dashed box regions in the left column. (d) Optical lock-in detection imaging (OLID) was performed on the same sample with three switching cycles. While the image contrast of weak signals was greatly improved (arrows), OLID was less sensitive to the subtle switching rate difference between the cytoplasm and cell nucleus. (e) The signal profiles along the dashed lines in (c–d), showing the improvement in lateral resolution and cytoplasm-nucleus contrast by rsPIM.

and thus from depths closer to the focal plane. As shown in Fig. 3(d), compared with conventional microscopy image, the rsPIM image shows significantly reduced out-of-focus signals.

To further study the rsPIM performance in imaging live cells, mammalian HeLa cells were transiently transfected with plasmids encoding rsTagRFP fusion proteins. Histone H2B in cell nucleus and β-actin in cytoplasm fused to rsTagRFP were imaged by both confocal microscopy and rsPIM. As before, three switching cycles were performed, and the expressed rsTagRFP in live cells could be stably switched on and off. The switching dynamics were extracted in the rsPIM. Compared with confocal microscopy, the improved resolution of rsPIM is shown by both the rsTagRFP-H2B [Figs. 4(a) and 4(b)] and rsTagRFP-β-actin [Figs. 4(c) and 4(d)] images. In particular, three neighboring β-actin fibers can be distinguished in the rsPIM image but not in the confocal image [Fig. 4(d)]. The mean measured diameter of the β-actin fiber is about 500 nm, consistent with the literature.[30] Compared with confocal microscopy, autofluorescence signals from the background were better rejected in the rsPIM, because they could not be switched off as rsTagRFP.

5 Discussion

RsPIM provides a method for subdiffraction imaging of synthetic or genetically encoded optical switches, and combines easy implementation on conventional confocal microscopy. This approach relies on the specific properties of the optical switches: their fluorescence emission can be switched on and off, and the switching rates depend on the excitation intensity. These properties immediately produce four advantages: (1) the background autofluorescence signals, which typically do not possess such switching capabilities, and thus can be easily removed, resulting in improved cell-to-background contrast,

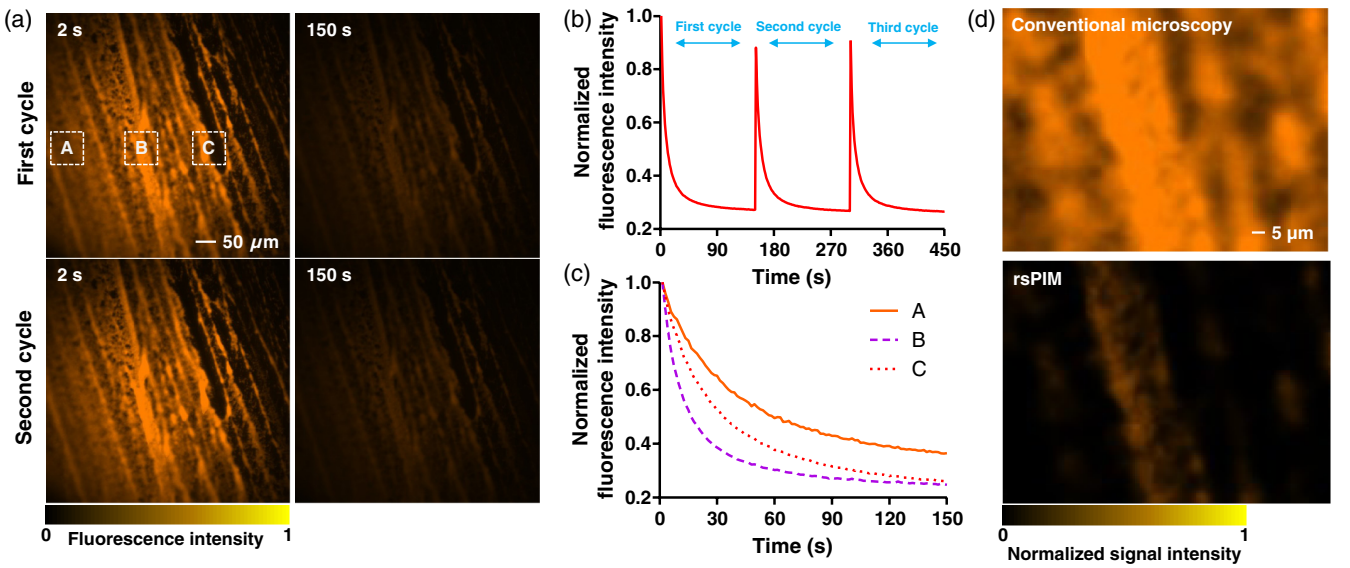

Fig. 3 Reversibly switchable photo-imprint microscopy (rsPIM) of live bacterial cells expressing rsTagRFP. (a) Conventional microscopy image of streaks of LMG194 bacterial cells expressing rsTagRFP, showing the switching capability of rsTagRFP. (b) Time course of averaged switching dynamics of rsTagRFP for three cycles. (c) Switching-off time courses of rsTagRFP at three representative regions, where Region B is in focus and Regions A and C are out of focus. It is clear that Region B has a faster switching rate than Regions A and C. (d) Comparison of conventional microscopy and rsPIM in optical sectioning. Taking advantage of the inhomogeneous axial excitation intensity distribution, rsPIM can efficiently block the out-of-focus signals.

(2) fluorophores in the central region of the excitation volume are switched off faster than those in the periphery due to the Gaussian light intensity distribution. Nonlinear signal dependence on the excitation intensity can be extracted from the switching dynamics, providing enhanced lateral resolution, (3) similarly, due to the nonuniform axial light intensity distribution, fluorophores in the focal plane are switched off at a faster rate than those out of focus. Nonlinear fitting of the switching dynamics can block more out-of-focus signals, and thus improve the optical sectioning, and (4) the fluorophores switched off can be switched on at the end of each cycle, resulting in lossless imaging. Thus, images can be acquired many times for longitudinal studies.

Capitalizing on these advantages, rsPIM has achieved subdiffraction imaging of reversibly switchable dyes and fluorescent proteins. This method does not need system modifications to the existing commercial fluorescence microscopes, and thus can potentially be adapted by regular cell biological laboratories. The principle of rsPIM can be transferred to two-photon microscopy and the mainstream optical imaging tool for neuroscience studies. The switching rate has a power dependence of at least two in two-photon absorption, and two-photon rsPIM should have a more pronounced resolution improvement over one-photon rsPIM. Because photoswitching occurs in the excitation phase of the imaging process, our method can be potentially applied to photoacoustic microscopy, where the laser-induced acoustic waves are detected by a focused ultrasonic transducer.[31,32] Since the resolution enhancement gained from the photoswitching dynamics is complementary to other subdiffraction mechanisms, the principle of rsPIM has the potential to be incorporated into other methods to further improve their resolutions.[2,6,33] Basically, all reversibly switchable fluorophores can be used for rsPIM. Particularly, switchable fluorophores with a strong photobleaching tolerance and short switching life times are preferred. Since rsPIM mainly needs repeated scanning and simple mathematic fitting, an add-on function can be incorporated into the original software of standard microscopes.

The current rsPIM has two major issues that need to be addressed in the future. First, the resolution improvement is still not as significant as that of RESOLFT and (F)PALM/STORM. With a linear switching rate dependence on the excitation intensity, it will be challenging for rsPIM to achieve a spatial resolution similar to STORM. To address this issue, other switching dynamics with higher order dependence may help to enhance the resolution improvement. Alternatively, a higher order polynomial fitting can be used provided there is a sufficient SNR. Second, the imaging speed is not fast enough for a real-time dynamic study. The current rsPIM typically completes a switching cycle in tens to hundreds of seconds, too slow for most biological dynamic processes. To address this issue, the excitation intensity can be increased, with the increased risk of permanent photobleaching. Reducing the field of view or using light-sheet illumination may also be used to accelerate the imaging speed.

Here, we need to emphasize that rsPIM is a subdiffraction imaging method with only a moderate improvement in imaging performance, while simplicity is its most significant feature. However, it is constructive to compare the rsPIM with other imaging methods utilizing rsFPs, which set to improve the spatial resolution and/or image contrast (Table 1). Compared with RESOLFT and (F)PALM/STORM, rsPIM has a lower spatial resolution but less system complexity or data processing. Compared with OLID, rsPIM can not only block the out-of-focus signals, but also improve the spatial resolution. However, rsPIM is less sensitive to weak fluorescence signals than OLID. Compared with pcSOFI, rsPIM has not only a lower resolution and longer imaging time, but also less computation intensity. Compared with MPDI/MPAI, rsPIM should be able to achieve

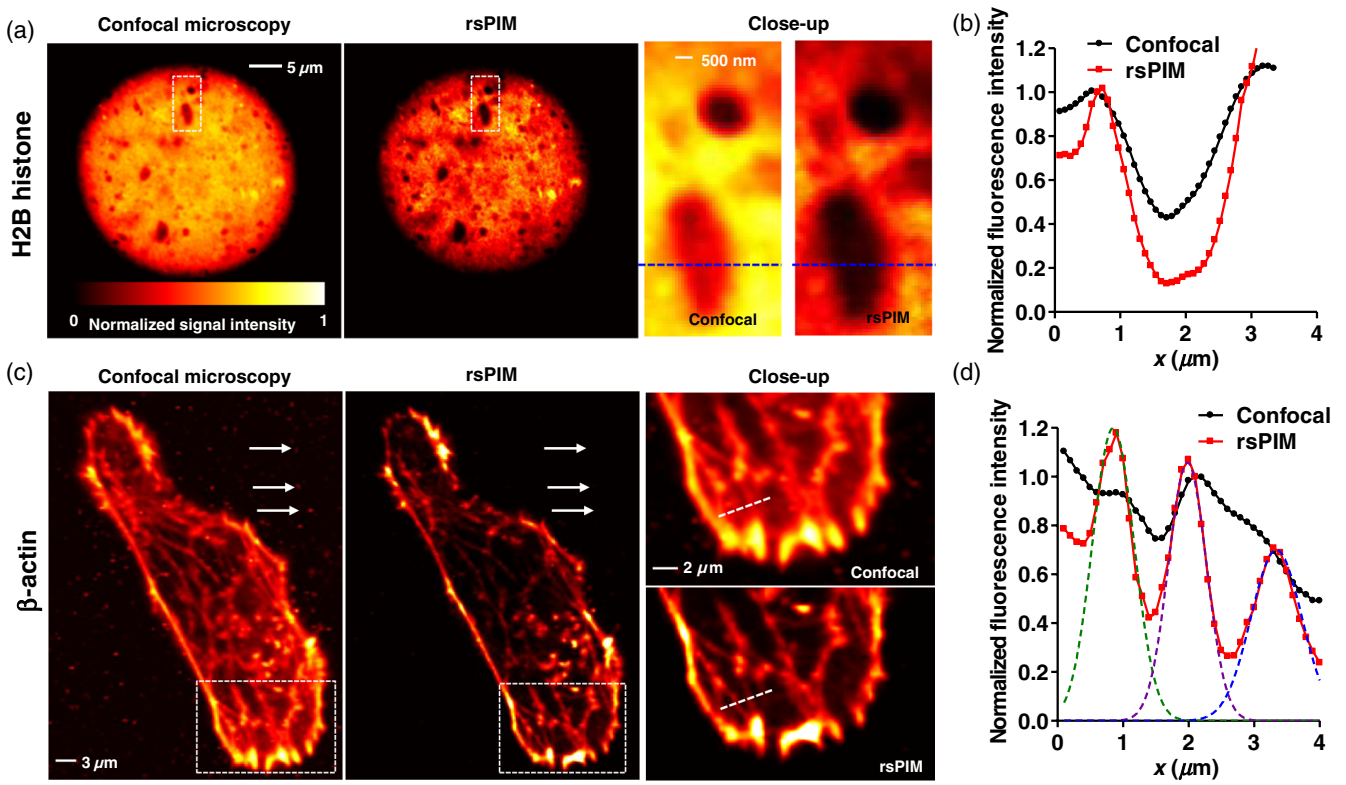

Fig. 4 Reversibly switchable photo-imprint microscopy (rsPIM) of live mammalian cells expressing rsTagRFP. (a) Comparison of confocal microscopy and rsPIM of the HeLa epithelial cells transiently transfected with the rsTagRFP-H2B fusion. The close-up images show magnified views of the regions marked by dashed boxes. rsPIM can provide sharper features than confocal microscopy. (b) Signal profiles along the dashed lines in the close-up images in (a). (c) Confocal microscopy and rsPIM of the HeLa cells expressing the rsTagRFP-β-actin fusion. rsPIM images show superior resolution (close-up images) and efficient elimination of the background autofluorescence signals (arrows). (d) Signal profiles along the dashed lines in the close-up images in (c), where three neighboring β-actin fibers can be clearly discerned by rsPIM but not by confocal microscopy. The dashed lines are Gaussian fittings of the signal profiles, showing an average fiber diameter of ~500 nm.

Table 1 Comparison of the fluorescence imaging techniques that utilize reversibly switchable photo-imprint microscopy (rsFPs).

Imaging parameter	rsPIM	RESOLFT[5]	(F)PALM/STORM[7,8,9]	OLID[24]	MPDI/MPAI[25]	pcSOFI[23]
Lateral resolution (nm)	~100–150	~30–50	~10–50	~250	~250	~80–120
Axial resolution (nm)	~250	~30–600	~10–50	~400–500	~300–400	~200–300
Image contrast enhancement	High	High	High	Mixed[a]	High	High
Speed	Low	High	Low	Low	High	Medium
Excitation power	Low	Low	Low	Low	High	Low
Complexity of imaging setup	Low	High	Low	Low	Low	Low
Intensity of data processing	Low	Low	High	Low	Low	Medium

[a]High for the contrast enhancement between nonswitchable autofluorescence and switchable fluorescence signals, but low for the contrast enhancement between in-focus and out-of-focus signals.

better image contrast enhancement, because MPDI/MPAI is equivalent to the first-order two-photon rsPIM, although spatial resolution enhancement has not been demonstrated by MPDI/MPAI.

In conclusion, we expect that rsPIM will become accessible to biological laboratories where confocal microscopy or two-photon microscopy are routinely used. Although the spatial resolution has not reached that achieved by STORM, with enhanced resolution and image contrast, rsPIM can be applied to efficiently image the cellular membranes and organelles, subcellular cytoskeletal and nuclear structures, large protein complexes and chromosomes in live mammalian cells.

Acknowledgments

The authors appreciate the close reading of the manuscript by Professor James Ballard. We thank Lidai Wang, Konstantin Maslov, and Liren Zhu for helpful discussions. This work was supported in part by the Grant Nos. EB016986 (NIH Director's Pioneer Award), R01 CA186567 (NIH Director's Transformative Research Award), S10 RR028864, and CA159959 (to L.V.W.), and GM073913 and CA164468 (to V.V.V.) from the National Institutes of Health.

References

1. B. Huang, M. Bates, and X. W. Zhuang, "Super-resolution fluorescence microscopy," *Annu. Rev. Biochem.* **78**, 993–1016 (2009).
2. K. I. Willig et al., "STED microscopy reveals that synaptotagmin remains clustered after synaptic vesicle exocytosis," *Nature* **440**(7086), 935–939 (2006).
3. J. Humpolickova, A. Benda, and J. Enderlein, "Optical saturation as a versatile tool to enhance resolution in confocal microscopy," *Biophys. J.* **97**(9), 2623–2629 (2009).
4. J. Humpolickova et al., "Dynamic saturation optical microscopy: employing dark-state formation kinetics for resolution enhancement," *Phys. Chem. Chem. Phys.* **12**(39), 12457–12465 (2010).
5. M. Hofmann et al., "Breaking the diffraction barrier in fluorescence microscopy at low light intensities by using reversibly photoswitchable proteins," *Proc. Natl. Acad. Sci. U. S. A.* **102**(49), 17565–17569 (2005).
6. M. G. L. Gustafsson, "Nonlinear structured-illumination microscopy: wide-field fluorescence imaging with theoretically unlimited resolution," *Proc. Natl. Acad. Sci. U. S. A.* **102**(37), 13081–13086 (2005).
7. E. Betzig et al., "Imaging intracellular fluorescent proteins at nanometer resolution," *Science* **313**(5793), 1642–1645 (2006).
8. S. T. Hess, T. P. Girirajan, and M. D. Mason, "Ultra-high resolution imaging by fluorescence photoactivation localization microscopy," *Biophys. J.* **91**(11), 4258–4272 (2006).
9. M. J. Rust, M. Bates, and X. W. Zhuang, "Sub-diffraction-limit imaging by stochastic optical reconstruction microscopy (STORM)," *Nat. Methods* **3**(10), 793–795 (2006).
10. J. Yao et al., "Photoimprint photoacoustic microscopy for three-dimensional label-free subdiffraction imaging," *Phys. Rev. Lett.* **112**(1), 014302 (2014).
11. C. Li et al., "Optical sectioning by wide-field photobleaching imprinting microscopy," *Appl. Phys. Lett.* **103**(18), 183703 (2013).
12. L. Gao et al., "Photothermal bleaching in time-lapse photoacoustic microscopy," *J. Biophoton.* **6**(6–7), 543–548 (2013).
13. L. Gao et al., "Photobleaching imprinting microscopy: seeing clearer and deeper," *J. Cell Sci.* **126**(23), 142943 (2013).
14. D. M. Shcherbakova, O. M. Subach, and V. V. Verkhusha, "Red fluorescent proteins: advanced imaging applications and future design," *Angew. Chem. Int. Ed.* **51**(43), 10724–10738 (2012).
15. A. Miyawaki, D. M. Shcherbakova, and V. V. Verkhusha, "Red fluorescent proteins: chromophore formation and cellular applications," *Curr. Opin. Struct. Biol.* **22**(5), 679–688 (2012).
16. R. Ando, H. Mizuno, and A. Miyawaki, "Regulated fast nucleocytoplasmic shuttling observed by reversible protein highlighting," *Science* **306**(5700), 1370–1373 (2004).
17. T. Grotjohann et al., "Diffraction-unlimited all-optical imaging and writing with a photochromic GFP," *Nature* **478**(7368), 204–208 (2011).
18. F. V. Subach et al., "Red fluorescent protein with reversibly photoswitchable absorbance for photochromic FRET," *Chem. Biol.* **17**(7), 745–55 (2010).
19. S. Pletnev et al., "A structural basis for reversible photoswitching of absorbance spectra in red fluorescent protein rsTagRFP," *J. Mol. Biol.* **417**(3), 144–151 (2012).
20. S. Habuchi et al., "Reversible single-molecule photoswitching in the GFP-like fluorescent protein Dronpa," *Proc. Natl. Acad. Sci. U. S. A.* **102**(27), 9511–9516 (2005).
21. M. Bossi et al., "Multicolor far-field fluorescence nanoscopy through isolated detection of distinct molecular species," *Nano Lett.* **8**(8), 2463–2468 (2008).
22. G. T. Dempsey et al., "Evaluation of fluorophores for optimal performance in localization-based super-resolution imaging," *Nat. Methods* **8**(12), 1027–1036 (2011).
23. P. Dedecker et al., "Widely accessible method for superresolution fluorescence imaging of living systems," *Proc. Natl. Acad. Sci. U. S. A.* **109**(27), 10909–10914 (2012).
24. G. Marriott et al., "Optical lock-in detection imaging microscopy for contrast-enhanced imaging in living cells," *Proc. Natl. Acad. Sci. U. S. A.* **105**(46), 17789–17794 (2008).
25. Y. T. Kao et al., "Focal switching of photochromic fluorescent proteins enables multiphoton microscopy with superior image contrast," *Biomed. Opt. Express* **3**(8), 1955–1963 (2012).
26. F. V. Subach et al., "Red fluorescent protein with reversibly photoswitchable absorbance for photochromic FRET," *Chem. Biol.* **17**(7), 745–755 (2010).
27. Olympus America Inc., "Olympus fluoview FV1000 brochure" http://www.olympusamerica.com/files/seg_bio/fv1000_brochure.pdf (24 July 2014).
28. J. Enderlein, "Breaking the diffraction limit with dynamic saturation optical microscopy," *Appl. Phys. Lett.* **87**(9), 097105 (2005).
29. Y. L. Yan et al., "Reversible optical control of cyanine fluorescence in fixed and living cells: optical lock-in detection immunofluorescence imaging microscopy," *Philos. Trans. R. Soc. Lond. B Biol. Sci.* **368**(1611), 20120031 (2012).
30. H. Chang et al., "A unique series of reversibly switchable fluorescent proteins with beneficial properties for various applications," *Proc. Natl. Acad. Sci. U. S. A.* **109**(12), 4455–4460 (2012).
31. L. H. V. Wang and S. Hu, "Photoacoustic tomography: in vivo imaging from organelles to organs," *Science* **335**(6075), 1458–1462 (2012).
32. J. Yao and L. V. Wang, "Photoacoustic tomography: fundamentals, advances and prospects," *Contrast Media Mol. Imaging* **6**(5), 332–345 (2011).
33. M. Bates et al., "Multicolor super-resolution imaging with photoswitchable fluorescent probes," *Science* **317**(5845), 1749–1753 (2007).

Junjie Yao received his BS and MS degrees in biomedical engineering from Tsinghua University and completed his PhD degree at Washington University in St. Louis in 2012. Currently he is a research associate at Washington University, under the supervision of Dr. Lihong V. Wang. His research interests include the development of novel biomedical imaging techniques including photoacoustic imaging, optical imaging, and ultrasonic imaging.

Daria M. Shcherbakova is a postdoctoral research fellow in the laboratory of Dr. Verkhusha. Her research interests include the design of fluorescent probes and molecular biosensors and their application.

Chiye Li received his BS degree in life sciences in 2011 from the University of Science and Technology of China in Hefei, China. Currently he is a PhD student in biomedical engineering at Washington University in St. Louis. His research interests include the application of photoacoustic imaging in biological and medical studies.

Arie Krumholz is a postdoctoral researcher under the Cardiovascular Biology Training Grant at the Department of Biomedical Engineering at Washington University in St. Louis. Currently he is studying voltage-gated ion-channel structure and function. During his PhD with professor Lihong Wang, he focused on molecular imaging and demonstrated the suitability of many genetically encoded contrast agents for use with photoacoustic tomography, a novel imaging technique which combines optical illumination and acoustic detection.

Ramon A. Lorca received his BSc degree in biological sciences from P. Catholic University of Chile in 2001 and completed his PhD degree in biological sciences at P. Catholic University of Chile in 2008. He started his postdoctoral training at the Mohapatra Lab in the Department of Pharmacology, University of Iowa, from January 2009 to May 2010. He joined Dr. England's lab in May 2010 as a postdoctoral fellow.

Erin Reinl received her BS degree in 2009 from St. Norbert College in De Pere, Wisconsin. She worked as a research assistant in the Department of Biochemistry at the University of Iowa from May 2009 to July 2010. She joined Dr. England's lab at the University

of Iowa in May 2011 and transferred to Washington University Molecular and Cellular Biology Program in January of 2012 to complete her doctoral training.

Sarah K. England is a professor of OB/GYN at Washington University in St. Louis. Her basic science research focuses on the molecular mechanisms underlying uterine function during pregnancy. She has written many research and review articles and has reviewed for multiple journals in both basic science and clinical fields. She serves on review committees for multiple funding agencies including the NIH, AHA, and the Howard Hughes Medical Institute.

Vladislav V. Verkhusha is a professor at the Albert Einstein College of Medicine in New York. His research interests include the development of fluorescent probes, biosensors, high-through screening, and imaging approaches.

Lihong V. Wang is the Gene K. Beare Distinguished Professorship at Washington University. His laboratory invented functional photoacoustic tomography and three-dimensional (3-D) photoacoustic microscopy. He serves as the editor-in-chief of the *Journal of Biomedical Optics*. He was awarded OSA's C.E.K. Mees Medal, NIH Director's Pioneer Award, and IEEE's Biomedical Engineering Award.